International Journal of Hygiene and Environmental Health 264 (2025) 114523

Contents lists available at ScienceDirect

International Journal of Hygiene and Environmental Health

journal homepage: www.elsevier.com/locate/ijheh

Incidental nanoparticle characterisation in industrial settings to support risk assessment modelling

Verónica Moreno-Martín [a,b,*], Maria López [a], David Bou [g], Sónia Fraga [d,e,f,g], João Paulo Teixeira [d,e,f], Ana López-Lilao [h], Vicenta Sanfélix [h], Eliseo Monfort [h], Mar Viana [c,a]

[a] Institute of Environmental Assessment and Water Research – Spanish Research council (IDAEA-CSIC), Barcelona, 08034, Spain
[b] Barcelona University, Chemistry Faculty, Programa de doctorat de Química analítica i medi ambient, C/ de Martí i Franquès, 1-11, 08028, Barcelona, Spain
[c] Spanish Ministry of Ecological Transition, Pollution Prevention Unit, Pza. San Juan de la Cruz 10, 28071, Madrid, Spain
[d] Department of Environmental Health, National Institute of Health Dr. Ricardo Jorge, Porto, Portugal
[e] EPIUnit-Institute of Public Health, University of Porto, Porto, Portugal
[f] Laboratory for Integrative and Translational Research in Population Health (ITR), Porto, Portugal
[g] Department of Biomedicine, Unit of Pharmacology and Therapeutics, Faculty of Medicine, University of Porto, Porto, Portugal
[h] Institute of Ceramic Technology (ITC- AICE) - Universitat Jaume I, Av. Vicent Sos Baynat s/n, 12006 Castellón, Spain

ARTICLE INFO

Keywords:
Ultrafine particles
Incidental nanoparticles
Human exposure
In vitro testing
Health and safety
Risk management models
RMM

ABSTRACT

Research on nanoparticle (NP) release and potential exposure can be assessed through experimental field campaigns, laboratory simulations, and prediction models. However, risk assessment models are typically designed for manufactured NP (MNP) and have not been adapted for incidental NP (INP) properties. A notable research gap is identifying NP sources and their chemical, physical, and toxicological properties, especially in real-world settings. This work aims to provide insights into the release and physico-chemical properties of INP while contributing to improving models for INP release. INP release was evaluated through a case study in a ceramic tile firing facility, where aerosol (10 nm - 10 μm) properties were determined. The Control Banding (CB) Nanotool model was applied to test outputs based on provided input parameters.

Results: demonstrate the constant generation and release of INP during tile firing, with NP concentrations up to 68711/cm^3 and mean diameters of 37 nm, with 95% smaller than 100 nm. Particle morphology was mostly spherical, suggesting nucleation from precursor gases as the main formation mechanism. INP chemical composition was driven by primary ceramic components, while trace elements like Ni and Ti exhibited size-dependent patterns. In vitro cell viability tests indicated low to medium cytotoxicity of PM_2 aerosols, decreasing human alveolar epithelial cell viability in a concentration-dependent manner. Applying the risk model with varying input parameters revealed that the risk level (RL) based on severity scores decreased when aerosol size distribution data were used, illustrating the model's sensitivity to input variables.

We conclude on the need for comprehensive experimental datasets to support risk assessment models and achieve effective risk management strategies in real-world scenarios.

1. Introduction

Personal exposure to ultrafine (UFP) and nanoparticles (NP; <100 nm) is becoming a growing concern in outdoor and indoor environments, due to their well-known health impacts (Oberdörster, 2001; Pope III & Dockery, 2006; Lelieveld et al., 2015; Bakand and Hayes, 2016; Bain et al., 2024). Specifically, in recent years, research focused on assessing exposure to NP across different industrial and occupational settings, from hair salons (Kaikiti et al., 2022) or 3D printing (Stefaniak et al., 2018; Zhang et al., 2018; Bernatikova et al., 2021; Romanowski et al., 2023) to shipyard operations (López et al., 2022), thermal spraying (Viana et al., 2017; Salmatonidis et al., 2019; Darut et al., 2021; Afshari et al., 2022; Bessa et al., 2022) and welding processes (Berger et al., 2021). In these kinds of settings, released NP may be originated from manufactured (MNP) or incidentally formed (INP) (Van Broekhuizen et al., 2012; Viitanen et al., 2017; Sousa et al., 2021).

* Corresponding author. Institute of Environmental Assessment and Water Research – Spanish Research council (IDAEA-CSIC), Barcelona, 08034, Spain.
E-mail address: veronica.moreno@idaea.csic.es (V. Moreno-Martín).

https://doi.org/10.1016/j.ijheh.2025.114523
Received 7 October 2024; Received in revised form 28 December 2024; Accepted 15 January 2025
Available online 25 January 2025

NP release and potential exposure impacts can be determined by means of experimental field campaigns, laboratory simulations and/or predictive modelling. The former two can provide data on metrics such as particle number concentration or particle size distribution, which can then be used to create and/or feed prediction models. While predictive models for urban-scale aerosol dispersion and NP dispersion prediction are highly developed, for example the Multicomponent Aerosol Formation (MAFOR) (Karl et al., 2022), (AEROFOR) (Markku and Pirjola, 2001), Water Research and Forecasting Model (WRF) (UCAR, 2024) or the Copernicus Atmosphere Monitoring Service (CAMS) (Copernicus, 2024), the literature on models for industrial applications, such as the Stoffenmanager Nano (Marquart et al., 2008; Van Duuren-Stuurman et al., 2012), ART (Fransman et al., 2011), CB Nanotool (Paik et al., 2008; Zalk et al., 2009) or the NanoSafer CB-tool (Jensen et al., 2013) is significantly scarcer, in particular regarding model validation in industrial settings. Furthermore, these models are designed to estimate the occupational risk of manufactured nanoparticles (MNPs), and they have so far not been specifically designed to reproduce INP concentrations and properties. Finally, although the European Chemicals Agency (ECHA) states that occupational exposure to inhalable chemicals can be assessed through modelling as an alternative or to complement workplace monitoring, these methods have not yet been standardised or recognised by the regulatory institutions (ECHA, 2016; Koivisto et al., 2019; Koivisto et al., 2021; Koivisto et al., 2022; Schlüter et al., 2022). Whereas these models are currently used to study MNP (Sousa et al., 2021), their accuracy still requires improvement (Koivisto et al., 2022) to reproduce the complexity of personal exposures in industrial settings, where NP properties are highly variable (Tsai et al., 2009; Ribalta et al., 2019; Berger et al., 2021; López et al., 2023; Lovén et al., 2023; Salmatonidis et al., 2019b). One especially notable research gap is related to NP source identification as a determinant of NP chemical and physical properties (e.g., particle shape, size, surface area, and chemical composition), as these factors play a significant role in determining NP toxicity (Khadanga and Mishra, 2024; Sukhanova et al., 2018; Shin et al., 2015). However, the availability of comprehensive studies characterising a broad range of physical, chemical, and toxicological properties of NP in industrial settings is at present relatively limited; to the authors' knowledge studies available typically focus on either physical or chemical properties (Stone et al., 2010; Fonseca et al., 2015; Viana et al., 2017b; Salmatonidis et al., 2018; Ribalta et al., 2019; Salmatonidis et al., 2019a; Fonseca et al., 2021; Khadanga and Mishra, 2024) or describe NP toxicity under laboratory conditions (Kose et al., 2020; Bacova et al., 2022; Budagova et al., 2023; Matysiak-Kucharek et al., 2023; Rafieepour et al., 2023; Vaezi-Kakhki, 2023). As a result, indoor air NP models currently lack comprehensive databases for validation purposes (Liguori et al., 2016; Oomen et al., 2018).

In this framework, this work aims to provide insights into INP release and physico-chemical properties, with a focus on exposure and potential health risks, under real-world conditions with the ultimate goal to contribute to the improvement of NP indoor air modelling. To this end, NP release was evaluated following a case of study approach in a ceramic tile firing facility, where aerosol (10 nm - 10 μm) physical, chemical, morphological, and toxicological properties were determined. Subsequently, the CB Nanotool model (model V008), a qualitative risk assessment model previously applied to INP (Nasirzadeh et al., 2023; Silva et al., 2016; Zalk et al., 2019), was selected and applied with the aim to assess the influence of the input parameters in the model output (i.e. severity score).

2. Materials and methods

2.1. Particle emission scenario

The ceramic cluster of Castelló region is Spain's major ceramic tile producer (97 %), the largest producer in Europe together with the Italian ceramic cluster of Modena (Minguillón et al., 2014) and the 5th globally (Baraldi, 2023). Thus, ceramic production was selected as a relevant emission and exposure scenario. In addition, the facility selected was considered representative of this type of industrial activity in Europe.

The ceramic tile manufacturing process consists of various stages, which differ as a function of the product made. The main tile production stages are: the raw materials preparation, the tile forming, drying, glazing and decorating, and firing. The greatest energetic stage is firing where peak temperatures around 1150–1200 °C are typically required, and consumes 55% of all thermal energy used in ceramic tile manufacture.

The ceramic tile firing area was inside the selected factory and consisted of four kilns, all parallel to each other, used to fire white earthenware tiles, red earthenware tiles and porcelain stoneware tiles indistinctly (Fig. 2). Monitoring was carried out in kiln 4 as it was separated from the other kilns by an enclosure; this is a significant factor as, typically, in ceramic industry factories, the kilns are positioned in parallel and operate simultaneously. The wall separation from the other kilns enabled a more accurate characterisation of the specific NP emissions from this process, minimising the interference from other potential emission sources. The ceramic tile kiln assessed was a single-deck roller kiln (SACMI KMS 2500/109.2) 90 m long, operated with natural gas and air burners (at the heating and firing stages) below and above the roller plane on which ceramic tiles travel along the kiln. The studied kiln was formed by 43 modules, of 2.10 m long each. The rollers divided the kilns in two chambers, top and bottom, which could be set at different temperatures (Fig. 1).

The ceramic tile firing process involves three main steps. First, the unfired tiles enter the kiln and are heated from room temperature up to 600 °C. Then, during the firing stage, the temperature is raised up to 1200 °C. Finally, the tiles are cooled down from the peak to room temperature (Mezquita et al., 2014) (Fig. 1). The products being manufactured during the study were red earthenware tiles and porcelain stoneware tiles.

In these furnaces the combustion gases are evacuated through the chimney at the furnace entrance, but in the zone of maximum temperature the furnaces work under overpressure, so that, depending on the sealing of the furnace combustion chamber, some gases containing pollutants (products of combustion and thermal decomposition of the raw materials) may be released into the surroundings.

2.2. Particle monitoring and sampling

Aerosol monitoring was carried out during two different field campaigns on 11–13 May 2022 and 06–08 July 2022. A near field (NF)/far field (FF) approach (Koivisto et al., 2021a,b) was used to determine the monitoring locations, determining two near field positions 3 m away from the studied area representative of the emission source (ES) and 1 m far from the worker area (WA). In addition, and indoor background (BG) placed 30 m away from the kiln entrance was selected es FF location (Koivisto et al., 2021b).To determine the ES measuring point, an initial screening of the total particle number concentrations (N) was carried out using a DiSCMini particle counter (10–700 nm, Testo AG) (Fig. S1). The WA was located at the exit of the kiln, where workers carry out quality control operations, and the BG location was positioned distant from the ES and the WA (Fig. 2). During the experimental campaigns, particle number concentrations were monitored simultaneously at the ES, WA and BG locations with a DiSCmini particle counter. Aerosol monitoring and sampling were conducted simultaneously at the ES and the WA; particle number concentrations and size distribution were determined using a portable scanning mobility particle sizer (NanoScan SMPS, TSI Model 3910, USA), samples for morphological characterisation were collected on SEM grids Quantifolil® AU, and samples for toxicological characterisation were collected using an impinger (Biosampler SKC) at both locations. Samples for chemical characterisation were collected at the ES using an electrical low-pressure impactor (ELPI+) (Dekati, Finland) (Table 1). Both the DiSCmini and Nanoscan instruments have

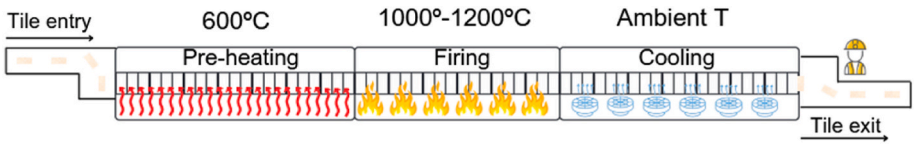

Fig. 1. Scheme of the kiln 4 and temperature phases.

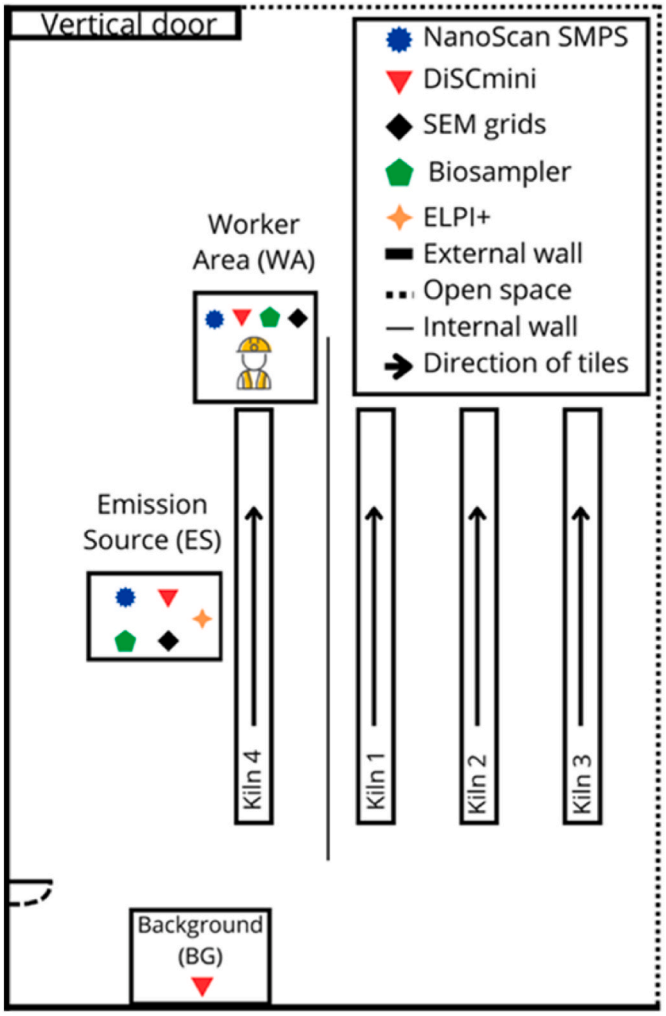

Fig. 2. Schematic view of the industrial plant.

certain limitations in terms of accuracy. The DiSCmini has an accuracy of approximately 30% (Testo DiSCmini manual, 2016). Similarly, the NanoScan, has an accuracy of 20 % (Ahlawat et al., 2022).

Various analytical techniques were employed to assess the physical, chemical, and toxicological properties of aerosols collected through different sampling methods. Chemical properties were determined for size-resolved aerosols. Samples were collected on polycarbonate filters using an ELPI+, covering a range from 6 nm to 10 μm across 15 stages. The filters were dissolved by acid digestion, then the resulting extract was analysed by inductively coupled plasma-atomic emission spectrometry (ICP-AES, Thermo Fisher Scientific, model iCAP 6500 Radial) and inductively coupled plasma-mass spectrometry (ICP-MS, model iCAP-RQ, Thermo Fisher Scientific, USA) (Querol et al., 2001).

The analysis of single particle morphology and composition was conducted by Scanning Electron Microscopy (SEM) (QUATTRO S, Thermo Fisher Scientific, USA) microscope coupled with an energy-dispersive X-ray (EDX) spectrometer (Pathfinder, Thermo Fisher Scientific, USA). Particles were collected on SEM grids Quantifolil® AU grids with 1 μm diameter holes – 4 μm separation of 200 mesh). These grids were positioned in sampling cassettes (SKC INS, USA, inlet diameter 1/8 in, filter diameter 25 mm), following the sampling protocols outlined by (Tsai et al. (2009), Fonseca et al., 2015b and Ribalta et al. (2019a,b)). Subsequently, the cassettes were connected to an SKC Leland pump operating at a flow rate of 3 L/min.

Sampling of PM_2 aerosols for *in vitro* testing was conducted using an SKC BioSampler® connected to a sonic-flow BioLite + pump (12.5 L/min) during 30 min. The particles were collected in 20 mL-glass vessels containing serum-free DMEM (Dulbecco's modified Eagle's medium) with 100 U/mL of penicillin and 100 μg/mL streptomycin to prevent bacterial growth. Samples were transferred to 50 mL centrifuge tubes and stored at - 20 °C until analysis.

Subsequently, the potential impact of the PM_2 aerosols sampled on the cell viability of human alveolar epithelial A549 cells (American Type Culture Collection, USA) was evaluated using the Alamar Blue (AB) assay, following the methodology described by Davoren et al. (2007), and modified as outlined by López et al. (2022). For that purpose, cells were cultured in DMEM (Gibco-Thermo Fisher Scientific, USA) supplemented with 10% fetal bovine serum (FBS) (Gibco-Thermo Fisher Scientific, USA), 100 U/mL penicillin and 100 μg/mL streptomycin (Gibco-Thermo Fisher Scientific, USA), and maintained in a humidified cell incubator at 37 °C with 5% CO_2. For the cytotoxicity experiments, cells were seeded in 96-well plates (150 000 cells per well) and allowed to adhere for 48 h. A total of eight samples was collected during one day at two different locations (four at the worker area and four at the emission source) at four different timepoints, and cell viability after exposure for 24 h to three dilutions (1:2, 1:4 and 1:8) of the PM_2 aerosols collected was determined. Negative control (NC) cells were incubated with serum-free DMEM, while positive control (PC) cells were exposed to 70% ethanol (EtOH). After exposure, the medium was removed and 100 μl of the AB reagent diluted to 1:10 was added to each well and the cells were incubated for 3 h at 37 °C with 5% CO_2. Fluorescence was measured using a microplate reader (Molecular Devices SpectraMax® iD3, USA) set to an excitation and emission wavelengths of 570 nm and 610 nm, respectively. Measurements were performed in triplicate to ensure high precision and reliability. Finally, the data were normalised based on the mean value of the NC and expressed as percentage of NC.

Table 1
Instrumentation deployed (ES: Emission Source; WA: Worker Area).

Instrumentation	Range	Resolution	Parameter	Location
NanoScan SMPS (TSI Model 3910)	10–420 nm	1 min	Particle number and size distribution	ES-WA
DiSCmini (TESTO AG)	10–700 nm	1seg	Particle number concentration and mean diameter	ES-WA
Electrical Low Pressure Impactor (ELPI+)	6 nm–10 μm	Continuous	Size-resolved chemical characterisation	ES
BioSampler (SKC)	<2 μm	30 min	In vitro toxicity testing	ES-WA
SEM grids (Quantifolil) (SKC)	–	Continuous	Particle morphology	ES-WA

Results refer to the 10% inhibitory concentration (IC_{10}), which indicates the concentration of particles required to achieve 10 % inhibition of a biological process (Sebaugh, 2011).

2.3. Statistical analyses

The concentrations recorded in the WA were considered statistically significant following the approach described by Asbach et al. (2012):

Mean value during operation > BG + 3x < (sBG)

Where BG is the mean BG concentration during (pre-activity) and sBG is the standard deviation of the background concentration (Asbach et al., 2012).While this approach was originally designed and validated for particle number concentrations, it was subsequently also validated for particle mass concentrations (Ribalta et al., 2019a,b). In addition, the normality of the data was analysed by Kolmogorov-Smirnov test using SPSS Statistics 27. In case of normal distribution of the data, the parametric ANOVA test was performed to assess the significance of the datasets, while for the non-parametric data the Kruskal-Wallis test was applied.

Finally, statistical and nonlinear regression analyses of cell viability data were performed using GraphPad Prism 6 (GraphPad Software, Inc., USA). The 10% inhibitory concentration (IC10) values of the PM2 liquid samples in A549 cells was estimated from the AB concentration-response curves, fitted using a three-parameter log (inhibitor vs. normalised response model) using the least squares as fitting method. Kruskall-Wallis analysis was conducted to test significance vs control. Significance was accepted at a P value < 0.05 for all tests.

2.4. Control banding (CB) tool

An analysis was conducted to assess how the introduction of additional metrics, such as particle size distribution, influences the model outputs. The model selected for this test was the Control Banding (CB) Nanotool V008, developed at the Lawrence Livermore National Laboratory (USA) by (Paik et al., 2008; Zalk and Paik, 2009), which is a publicly available CB tool downloadable as macros excel sheet model at https://controlbanding.llnl.gov/download. This method was designed to assess the risk of exposure to engineered nanomaterials (ENM). Regardless, this method has been previously applied to INP (Silva et al., 2016; Paik et al., 2008; Nasirzadeh et al., 2023; Sousa et al., 2023), which is the main reason why this model was selected.

The model was implemented in two modes: the deterministic and the Monte Carlo model, which allows for the input of distributions for each material parameter. By incorporating parameter distributions, the Monte Carlo model enables a more accurate calculation of the risk level (RL), reflecting the variability and uncertainty inherent in the material properties.

The CB Nanotool assigns hazards and exposures into four bands each, representing severity and probability scores respectively, and identifies four risk level (RL) control bands. The overall RL is determined through a matrix that combines probability (columns) and severity (rows) scores, with a maximum combined score of 100, where 70 points are based on characteristics of the nanomaterial (NM) and the remaining 30 points on the characteristics of the parent material (PM). Based on these scores, a RL is assigned to one of the four control bands, which correspond to a specific control measure: RL 1 (General Ventilation), RL 2 (Fume Hood or Local Exhaust Ventilation), RL 3 (Containment), and RL 4 (Seek specialist advice). When a parameter is marked as unknown, it assigned a value equal to 75% of the maximum possible score, classifying the situation as RL 3 indicating the need for exposure containment (Table 2).

3. Results and discussion

3.1. Nanoparticle generation and release

Particle number concentrations (N) and mean diameter are reported in Fig. 3, and results show that they did not vary largely overtime. Particle number concentrations were higher in the ES (1-min average of 84210 ± 34947/cm^3) than in the WA (68711 ± 29641/cm^3), with similar mean diameters at both locations (ES = 37±3 nm, WA = 37±4 nm; Fig. 3), while BG levels were 11863 ± 4678/cm^3 with mean diameter 24±2 nm. The concentrations recorded were significantly higher than the BG of the facility (Asbach et al., 2012), and may be considered relatively high when compared with typical outdoor UFP concentrations in urban environments (Reche et al., 2011). Particle number concentrations in the ES were lower than previously reported values (8×10^5 and 1.6×10^5/cm^3 for a conventional old (10-years-old) and new advanced kiln (2-years-old), respectively (Salmatonidis et al., 2019). Emissions were also lower than those reported for other ceramic processes such as laser sintering ($6.2x10^5$/cm^3) (Fonseca et al., 2015a,b) or traditional pottery ($6.5x10^5$/cm^3) (Voliotis et al., 2014). The concentrations recorded in the WA were also lower than those reported in the literature for other ceramic processes such as laser sintering (3.6×10^5/cm^3 in the breathing zone) (Fonseca et al., 2015a,b) or atmospheric plasma spraying (up to 3.3×10^6/cm^3) (Viana et al., 2017a).

Overall, 95% of the particles showed mean diameters lower than 100 nm. Particle size distribution exhibited a unimodal pattern at the ES, with a mean diameter of 37 nm. Conversely, at the WA a bimodal distribution was observed, characterised by a smaller and a larger peak around 15 nm and 27 nm, respectively. The smaller mode detected in the WA (and not in the ES) was interpreted as resulting from new particle formation from precursor gases emitted in the ES and transferred to the WA, where they cooled down and formed new particles by nucleation. The 27 nm mode was detected at both locations and was interpreted as direct NP emissions from the kiln. The fact that the impact of these newly formed particles was not observed on the mean diameter in the WA is probably result of instrumental accuracy, given the relative low contribution of this aerosol mode to the mean. SEM analysis data aligns with this result evidencing that particles collected at the WA were smaller than those collected at the ES and also revealed aggregates of spherical NP in the WA (Fig. 4). Actually, in both locations particles exhibited a predominantly spherical shape, indicative of a high-temperature formation process (Salmatonidis et al., 2018) (Fig. 5). These results agree with prior research in terms of mean diameter of NP from ceramic tile firing processes: 75% of particles exhibited sizes below 50 nm, with 40% being smaller than 30 nm in a ceramic tile facility

Table 2
Maximum points per factor for probability and severity scores.

Probability factor	Maximum points	Severity factor	Maximum points	Severity factor	Maximum points
Amount of chemical (mg)	25	Surface reactivity	10	Asthmagen	6
Dustiness	30	Particle shape (NM)	10	Toxicity (PM)	10
Number of employees	15	Particle diameter (NM)	10	Carcinogenicity (PM)	4
Frequency of operation	15	Solubility (NM)	10	Reproductive toxicity (PM)	4
Operation duration	15	Carcinogenicity (NM)	6	Mutagenicity (PM)	4
		Reproductive toxicity (NM)	6	Dermal toxicity (PM)	4
		Mutagenicity (NM)	6	Asthmagen (PM)	4
		Dermal toxicity (NM)	6		

PM - Parent material NM – Nanomaterial.

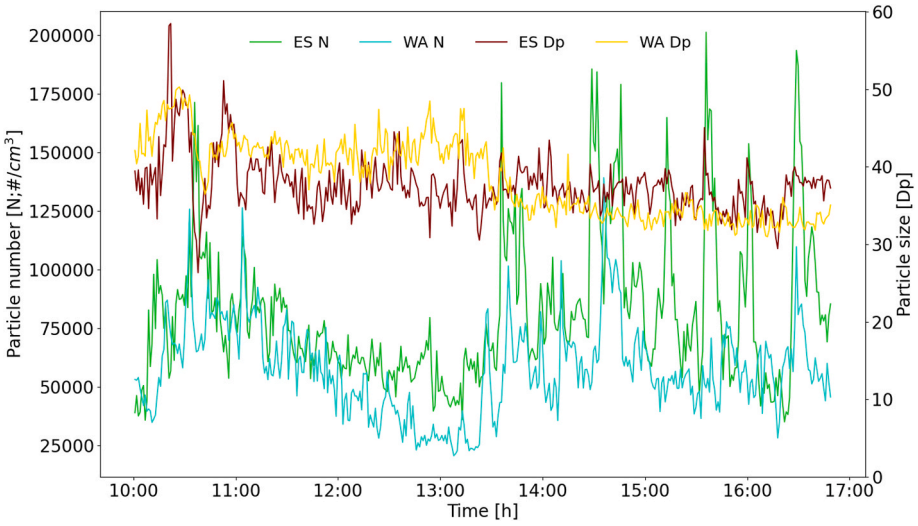

Fig. 3. Example of particle number concentrations recorded during one representative shift (July 06, 2022) monitored by Nanoscan SMPS.

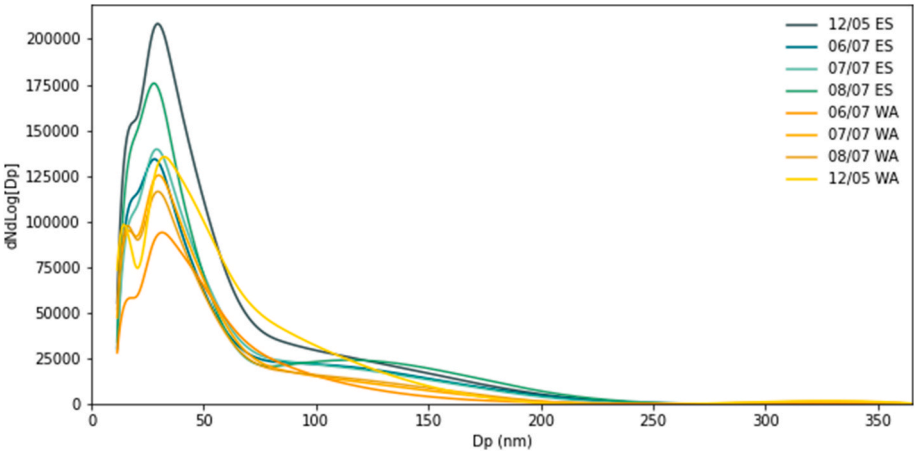

Fig. 4. Mean particle size distribution at the emission source (ES) and at the worker area (WA) for each day during the full monitoring period.

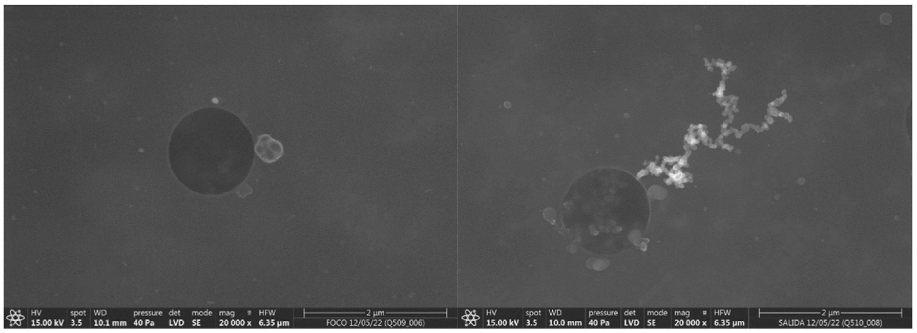

Fig. 5. Scanning Electron Microscopy (SEM) images of particles collected at the emission source (ES; left) and worker area (WA; right). Particles are the lighter-coloured elements.

(Salmatonidis et al., 2019) or those reported for traditional pottery, which ranged from 30 to 70 nm (Voliotis et al., 2014).

3.2. Size-dependent chemical fingerprint of the released particles

Chemical fingerprints, determined using a combination of SEM-EDX and chemical analysis of aerosols collected on ELPI + substrates, revealed that the finest aerosol size fractions (0.0156 μm) contained tracers such as Ti (<1 %), which increased in relative terms with increasing particle size (52 % in size fractions >0.257 μm). Conversely, the relative contribution of other trace elements such as Ni decreased with increasing particle size (33 % at 0.0156 μm–12 % at 0.095 μm). Thus, specific chemical properties evidenced a marked particle size dependence (Fig. 6). Minor components detected may have originated from glaze components (mainly frits and pigments), essentially composed of Ti, Cr, Ni and Zn (Almendro-Candel and Jordán Vidal,

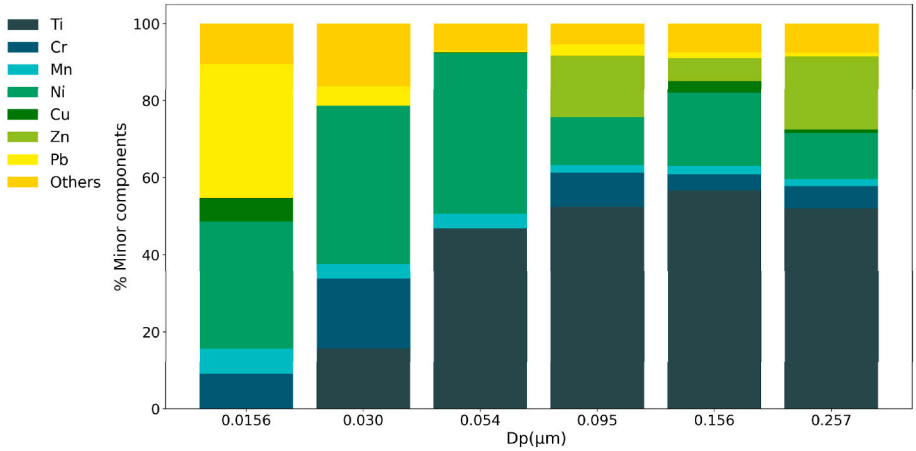

Fig. 6. Size-resolved chemical profile of trace elements in the ultrafine fraction of aerosols collected at the emission source (ES) location with an ELPI + impactor.

2024). The size-aggregated composition of the minor components varied with particle size.

Major components, on the other hand, showed mostly similar relative contributions to mass concentrations across all size fractions (Fig. S2).

SEM-EDX analysis indicated that composition and morphology of the ultrafine fraction of the aerosols collected in the ES was similar to that in the WA. The predominant composition consisted of typical ceramic materials (Anufrik et al., 2016), such as aluminosilicates of alkali (Na^+ and K^+) and alkali earth (Ca^{2+}) (Table S4). Na^+ appeared as the primary component across all fractions, ranging from 26 to 64 %, followed by Ca^{2+}, which constituted a significant portion (10–30 %), both in form of aluminosilicate (Fig. S2).

3.3. *In vitro cytotoxicity testing of PM_2 aerosols in liquid suspension*

Viability of human alveolar epithelial A549 cells was assessed after exposure for 24 h to three different dilutions (1:8, 1:4 and 1:2) of the PM_2 liquid suspensions collected both in the WA and ES at different time-points (1, 2, 3 and 4) during the same shift.

As show in Fig. 7, human alveolar epithelial cells incubated for 24 h with the PM_2 samples collected at the ES did not exhibit significant changes in viability compared to the control cells. However, A549 cells exposed to the PM_2 samples collected at the WA showed a low to moderate concentration-dependent decrease in cell viability, though only significant in WA2- (67 and 85 %) and WA4 (86 %)-exposed cells.

Analysis of the concentration-response curves (Fig. S3) revealed that WA2 was more potent than the WA4 PM_2 sample as evidenced by the lower IC_{10} (Table 3) (1.25×10^{11} vs 1.95×10^{11} particles/mL).

Given the similarity in chemical properties between the PM_2 aerosols collected in the ES and WA, lower cell viability induced by the PM_2 WA samples can be attributed to the presence of the 15 nm mode in the WA,

Table 3
Concentration (particles/mL) and 10% inhibitory concentration (IC_{10}) values of the PM_2 liquid suspensions in human alveolar epithelial cells.

	Original suspension concentration (particles/mL)	10% inhibitory concentration (IC_{10})(particles/mL)
WA 1	10.2×10^{11}	2.17×10^{11}
WA 2	9.75×10^{11}	1.25×10^{11}
WA 3	12.8×10^{11}	4.27×10^{11}
WA 4	7.90×10^{11}	1.95×10^{11}
ES 1	10.8×10^{11}	N.A.
ES 2	10.9×10^{11}	N.A.
ES 3	10.8×10^{11}	6.49×10^{11}
ES 4	2.84×10^{11}	0.91×10^{11}

Original suspension concentration was determined by aerosol monitoring data curation. IC_{10} values determined by analysis of the Alamar Blue (AB) concentration–response curves that were fitted using a three-parameter (inhibitor vs. normalised response model). N.A.: Unable to estimate..

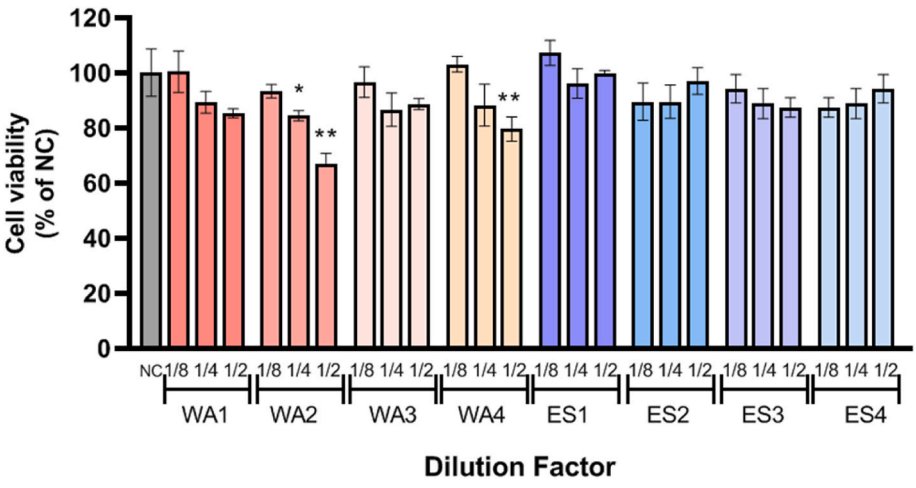

Fig. 7. Viability of human alveolar epithelial (A549) cells, after exposure for 24 h to the PM_2 liquid suspensions collected in the emission source (ES) and in the worker area (WA) during the shift. Data are expressed as mean ± standard deviation (n = 3, from one experiment). Values were normalised considering the negative control (NC). Data were analysed by Kruskal-Wallis analysis. *p < 0.05 vs. NC.

Table 4
Results obtained from application of the deterministic and Monte Carlo models of the CB Nanotool v2.0 for ceramic tile firing activities. Risk level and recommendations: RL 1 (General Ventilation), RL 2 (Fume Hood or Local Exhaust Ventilation), RL 3 (Containment), and RL 4 (Seek specialist advice).

	Severity		Probability		Overall risk level (RL)	Recommendation	Upgrade
	Score	Band	Score	Band			
Deterministic	64.5	High	76.25	Probable	RL4	Seek specialist advice	Yes
Monte-Carlo	61.6	High	76.2	Probable	RL4	Seek specialist advice	Yes

which were not detected in the PM_2 ES samples (Fig. 4). This aligns with prior research which evidenced that SiO_2 NP induce significant cytotoxic effects on A549 cells, showing a dose- and size-dependent correlation. Specifically, 6 nm NP exhibit a significant cytotoxic effect, with an IC_{50} value of 119.82 μg/ml (Tokgun et al., 2015). Furthermore, studies by Rafieepour et al. (2023) and Sushma et al. (2018) concluded that crystalline SiO_2 nanoparticles cause greater cell damage in A549 cells at concentrations exceeding 100 μg/mL compared to microparticles.

3.4. Risk assessment modelling

The CB Nanotool was used to assess the RL associated with tile firing activities with different sets of input parameters (Table S5). In the case of this model, which is a quantitative tool, the main difference was the inclusion (or exclusion) of particle size distribution data in the assessment. Initially, the deterministic model was applied. The results indicate that for the investigated activity, the severity score was in 64.5 points out of 100 and its probability score in 76.2 points. As a result, the RL was determined to be RL 4, recommending specialist consultation.

Subsequently, the Monte Carlo model was implemented, incorporating particle size distribution. The analysis revealed that the probability score (76.2) remained consistent across both models, whereas the severity score (61.6) demonstrated a slight decrease (Table 4). However, the RL classification remained at the highest level RL4. This result highlights that increasing knowledge about material characteristics and various exposure scenarios can affect the outcomes generated by the tool, in this case reducing exposure's severity while maintaining the overall risk classification. Our findings illustrate the potential variability in results when using the CB Nanotool, underscoring the importance of incorporating particle physico-chemical properties into CB tools for a more effective assessment and management of the workplace risks of INP.

4. Conclusions

The literature on indoor air NP emissions, especially in industrial environments, evidences a research gap in relation to model validation. Whereas data on the physical, chemical and toxicological properties of aerosols are reported separately in different studies, publications reporting comprehensive NP characterisations are relatively scarce. As a result, this limits the pool of studies available for testing and validation of risk assessment models (e.g., control banding tools). In order to address this research gap, the present study focused on NP emissions from ceramic tile firing, as a case study, to provide an in-depth characterisation of the physical, chemical, and toxicological properties of INP generated in this industrial process.

Results demonstrated the generation and release of INP at a relatively constant rate during the tile firing process, reading NP concentrations up to 68711/cm^3 (1-min mean) with mean diameters of 37 nm, in the WA, where 95% of the NP were <100 nm. Particle morphology was mostly spherical, suggesting that the main formation mechanism was nucleation from precursor gases. NP chemical composition was driven by the main components of the ceramic materials being fired (aluminosilicates), tracer elements were size dependent (e.g., the relative contribution from Ni increased from 0.0156 to 0.095 μm particles, whereas the opposite trend was observed for Ti). Finally, *in vitro* cell viability tests indicated no cytotoxicity of the ES PM_2 fraction and low/medium concentration-dependent cytotoxicity of the PM_2 fraction collected at the WA.

As a last stage of study, the severity level assessed by a control banding tool (in this case, CB Nanotool) regarding different sets of input parameters was tested. Whereas model outputs did not vary largely, our results evidence a decrease in risk severity of exposure to this kind of aerosols when specific data on aerosol size distribution were introduced as input parameter. Our findings illustrate the potential variability in results when using a qualitative tool such as the CB Nanotool, underscoring its significance in making informed decisions regarding nanoparticle exposure assessments.

Finally, the necessity for comprehensive experimental datasets of INP was highlighted, as current risk assessment models are not designed to assess risks derived from exposure to INPs.

CRediT authorship contribution statement

Verónica Moreno-Martín: Writing – original draft, Visualization, Methodology, Investigation, Formal analysis, Data curation, Conceptualization. **Maria López:** Writing – review & editing, Formal analysis. **David Bou:** Methodology, Formal analysis, Data curation. **Sónia Fraga:** Writing – review & editing, Formal analysis, Conceptualization. **João Paulo Teixeira:** Writing – review & editing. **Ana López-Lilao:** Writing – review & editing, Methodology. **Vicenta Sanfélix:** Writing – review & editing, Methodology. **Eliseo Monfort:** Writing – review & editing. **Mar Viana:** Writing – review & editing, Supervision, Resources, Methodology, Conceptualization.

Funding sources

Life NanoHealth (LIFE20 ENV-ES-000187)

This work was supported also by IVACE (Instituto Valenciano de Competitividad Empresarial). Project GAIA-IVACE (IMAMCA/2023/1)

Epidemiology Research Unit (EPIUnit) of the Institute of Public Health of the University of Porto (UIDB/04750/2020)

Associated Laboratory for Integrative and Translational Research in Population Health (ITR) (LA/P/0064/2020)

Acknowledgements

This work was carried out in the framework of project LIFE-NanoHealth (LIFE20 ENV-ES-000187). It was also supported by the Spanish Ministry of Science and Innovation (Project CEX2018-000794-S), by AGAUR (project 2017 SGR41) and by the Foundation for Science and Technology – FCT (Portuguese Ministry of Science, Technology and Higher Education) under the projects UIDB/04750/2020 and LA/P/0064/2020 with the DOI identifiers https://doi.org/10.54499/UIDB/04750/2020 and https://doi.org/10.54499/LA/P/0064/2020.

Appendix A. Supplementary data

Supplementary data to this article can be found online at https://doi.org/10.1016/j.ijheh.2025.114523.

References

Afshari, A.A., McKinney, W., Cumpston, J.L., Leonard, H.D., Cumpston, J.B., Meighan, T. G., Jackson, M., Friend, S., Kodali, V., Lee, E.G., Antonini, J.M., 2022. Development of a thermal spray coating aerosol generator and inhalation exposure system. Toxicol Rep 9, 126–135. https://doi.org/10.1016/j.toxrep.2022.01.004.

Ahlawat, A., Weinhold, K., Marval, J., Tronville, P., Leskinen, A., Komppula, M., Gerwig, H., Gerling, L., Weber, S., Jørgensen, R.B., Jensen, T.N., Merizak, M., Vogt, U., Ribalta, C., Viana, M., Schmitz, A., Chiesa, M., Gerosa, G., Keck, L., et al., 2022. Performance analysis of the NanoScan SMPS and the mini WRAS ultrafine aerosol particle size spectrometers. https://doi.org/10.5194/amt-2022-155.

Almendro-Candel, M.B., Jordán Vidal, M.M., 2024. Glasses, frits and glass-ceramics: processes and uses in the context of circular economy and waste vitrification. Coatings 14 (3). https://doi.org/10.3390/coatings14030346.

Anufrik, S.S., Kurian, N.N., Zhukova, I.I., Znosko, K.F., Belkov, M.V., 2016. Chemical composition of ceramic tile glazes. J. Appl. Spectrosc. 83 (5). https://doi.org/10.1007/s10812-016-0360-8.

Asbach, C., Kuhlbusch, T., Kaminski, H., Stahlmecke, B., Plitzko, S., Götz, U., Voetz, M., Kiesling, H.-J., Dahmann, D., 2012. Standard Operation Procedures for assessing exposure to nanomaterials, following a tiered approach. NanoGEM.

Bacova, J., Knotek, P., Kopecka, K., Hromadko, L., Capek, J., Nyvltova, P., Bruckova, L., Schröterova, L., Sestakova, B., Palarcik, J., Motola, M., Cizkova, D., Bezrouk, A., Handl, J., Fiala, Z., Rudolf, E., Bilkova, Z., Macak, J.M., Rousar, T., 2022. Evaluating the use of TiO 2 nanoparticles for toxicity testing in pulmonary A549 cells. https://doi.org/10.2147/IJN.S374955.

Bain, A., Vasdev, N., Tekade, M., Mishra, D.K., Sengupta, P., Tekade, R.K., 2024. Toxicity of nanomaterials. Public Health and Toxicology Issues Drug Research 2, 679–706. https://doi.org/10.1016/B978-0-443-15842-1.00023-5.

Bakand, S., Hayes, A., 2016. Toxicological considerations, toxicity assessment, and risk management of inhaled nanoparticles. In: International Journal of Molecular Sciences. MDPI AG. https://doi.org/10.3390/ijms17060929, 17, Issue 6.

Baraldi, L., 2023. World production and consumption of ceramic tiles. Ceramic World Review 153, 68. https://issuu.com/tiledizioni/docs/000_216_cwr_113.

Berger, F., Bernatíková, Š., Kocůrková, L., Přichystalová, R., Schreiberová, L., 2021. Occupational exposure to nanoparticles originating from welding – case studies from the Czech Republic. Med. Pr. 72 (3), 219–230. https://doi.org/10.13075/mp.5893.01058.

Bernatikova, S., Dudacek, A., Prichystalova, R., Klecka, V., Kocurkova, L., 2021. Characterization of ultrafine particles and VOCs emitted from a 3D printer. Int. J. Environ. Res. Publ. Health 18 (3), 1–15. https://doi.org/10.3390/ijerph18030929.

Bessa, M.J., Brandão, F., Fokkens, P.H.B., Leseman, D.L.A.C., Boere, A.J.F., Cassee, F.R., Salmatonidis, A., Viana, M., Monfort, E., Fraga, S., Teixeira, J.P., 2022. Unveiling the toxicity of fine and nano-sized airborne particles generated from industrial thermal spraying processes in human alveolar epithelial cells. Int. J. Mol. Sci. 23 (8). https://doi.org/10.3390/ijms23084278.

Budagova, S.O., Nadvodnyk, G.V., Belskaia, P.A., Obukhova, A.A., Lebedev, I.G., Osmanov, R.M., Dzhumaev, G.T., Agarzaev, M.M., 2023. Toxicity assessment of the selenium nanoparticles in vitro. J. Adv. Pharm. Educ. Res. 13 (3), 39–45. https://doi.org/10.51847/4i6JD9deHL.

Copernicus, 2024. Copernicus Atmosphere monitoring Service. https://atmosphere.copernicus.eu/.

Darut, G., Dieu, S., Schnuriger, B., Vignes, A., Morgeneyer, M., Lezzier, F., Devestel, F., Vion, A., Berguery, C., Roquette, J., Le Bihan, O., 2021. State of the art of particle emissions in thermal spraying and other high energy processes based on metal powders. J. Clean. Prod. 303. https://doi.org/10.1016/j.jclepro.2021.126952.

Davoren, M., Herzog, E., Casey, A., Cottineau, B., Chambers, G., Byrne, H.J., Lyng, F.M., 2007. In vitro toxicity evaluation of single walled carbon nanotubes on human A549 lung cells. Toxicol. Vitro 21 (3), 438–448. https://doi.org/10.1016/j.tiv.2006.10.007.

ECHA, 2016. Uidance on Information Requirements and Chemical Safety Assessment Chapter R.14: Occupational Exposure Assessment. Finland, Helsinki. https://echa.europa.eu/guidance-documents/guidance-on-information-requirements-and-chemical-safety-assessment.

Fonseca, A.S., Maragkidou, A., Viana, M., Querol, X., Hämeri, K., de Francisco, I., Estepa, C., Borrell, C., Lennikov, V., de la Fuente, G.F., 2015a. Process-generated nanoparticles from ceramic tile sintering: emissions, exposure and environmental release. Sci. Total Environ. 565, 922–932. https://doi.org/10.1016/j.scitotenv.2016.01.106.

Fonseca, A.S., Viana, M., Querol, X., Moreno, N., de Francisco, I., Estepa, C., de la Fuente, G.F., 2015b. Ultrafine and nanoparticle formation and emission mechanisms during laser processing of ceramic materials. J. Aerosol Sci. 88, 48–57. https://doi.org/10.1016/j.jaerosci.2015.05.013.

Fonseca, A.S., Viitanen, A.K., Kanerva, T., Säämänen, A., Aguerre-Chariol, O., Fable, S., Dermigny, A., Karoski, N., Fraboulet, I., Koponen, I.K., Delpivo, C., Villalba, A.V., Vázquez-Campos, S., Østerskov Jensen, A.C., Nielsen, S.H., Sahlgren, N., Clausen, P. A., Nguyen Larsen, B.X., Kofoed-Sørensen, V., et al., 2021. Occupational exposure and environmental release: the case study of pouring tio2 and filler materials for paint production. Int. J. Environ. Res. Publ. Health 18 (2), 1–26. https://doi.org/10.3390/ijerph18020418.

Fransman, W., Van Tongeren, M., Cherrie, J.W., Tischer, M., Schneider, T., Schinkel, J., Kromhout, H., Warren, N., Goede, H., Tielemans, E., 2011. Advanced reach tool (ART): development of the mechanistic model. Ann. Occup. Hyg. 55 (9), 957–979. https://doi.org/10.1093/annhyg/mer083.

Jensen, K.A., Saber, A.T., Kristensen, H.V., Koponen, I.K., Liguori, B., Wallin, Jensen, K. A., Saber, A.T., Kristensen, H.V., Koponen, I.K., Liguori, B., Wallin, 2013. NanoSafer vs. 1.1-Nanomaterial risk assessment using first order modeling. http://square.umin.ac.jp/nanoeh6/.

Kaikiti, C., Stylianou, M., Agapiou, A., 2022. TD-GC/MS analysis of indoor air pollutants (VOCs, PM) in hair salons. Chemosphere 294. https://doi.org/10.1016/j.chemosphere.2022.133691.

Karl, M., Pirjola, L., Grönholm, T., Kurppa, M., Anand, S., Zhang, X., Held, A., Sander, R., Dal Maso, M., Topping, D., Jiang, S., Kangas, L., Kukkonen, J., 2022. Description and evaluation of the community aerosol dynamics model MAFOR v2.0. Geosci. Model Dev. (GMD) 15 (9), 3969–4026. https://doi.org/10.5194/gmd-15-3969-2022.

Khadanga, V., Mishra, P.C., 2024. A review on toxicity mechanism and risk factors of nanoparticles in respiratory tract. Toxicology 153781. https://doi.org/10.1016/J.TOX.2024.153781.

Koivisto, A.J., Jayjock, M., Hämeri, K.J., Kulmala, M., Sprang, P. Van, Yu, M., Boor, B.E., Hussein, T., Koponen, I.K., Löndahl, J., Morawska, L., Little, J.C., Arnold, S., 2022a. Evaluating the theoretical background of STOFFENMANAGER® and the advanced REACH tool. Annals of Work Exposures and Health 66 (4), 520–536. https://doi.org/10.1093/annweh/wxab057.

Koivisto, A.J., Kling, K.I., Hänninen, O., Jayjock, M., Löndahl, J., Wierzbicka, A., Fonseca, A.S., Uhrbrand, K., Boor, B.E., Jiménez, A.S., Hämeri, K., Maso, M.D., Arnold, S.F., Jensen, K.A., Viana, M., Morawska, L., Hussein, T., 2019. Source specific exposure and risk assessment for indoor aerosols. Sci. Total Environ. 668, 13–24. https://doi.org/10.1016/j.scitotenv.2019.02.398.

Koivisto, A.J., Secco, B. Del, Trabucco, S., Nicosia, A., Ravegnani, F., Altin, M., Cabellos, J., Furxhi, I., Blosi, M., Costa, A., Lopez De Ipiña, J., Belosi, F., 2022b. Quantifying emission factors and setting conditions of use according to ECHA chapter R.14 for a spray process designed for nanocoatings-A case study. https://doi.org/10.3390/nano12040596.

Koivisto, A.J., Spinazzè, A., Verdonck, F., Borghi, F., Löndahl, J., Koponen, I.K., Verpaele, S., Jayjock, M., Hussein, T., Lopez de Ipiña, J., Arnold, S., Furxhi, I., 2021a. Assessment of exposure determinants and exposure levels by using stationary concentration measurements and a probabilistic near-field/far-field exposure model. Open Research Europe 1. https://doi.org/10.12688/openreseurope.13752.1.

Koivisto, A.J., Spinazzè, A., Verdonck, F., Borghi, F., Löndahl, J., Koponen, I.K., Verpaele, S., Jayjock, M., Hussein, T., Lopez De Ipiña, J., Arnold, S., Furxhi, I., 2021b. Assessment of exposure determinants and exposure levels by using stationary concentration measurements and a probabilistic near-field/far-field exposure model. https://doi.org/10.12688/openreseurope.13752.1 *[version 1; peer review: 2 approved]*.

Kose, O., Tomatis, M., Leclerc, L., Belblidia, N.B., Hochepied, J.F., Turci, F., Pourchez, J., Forest, V., 2020. Impact of the physicochemical features of TiO2Nanoparticles on their in vitro toxicity. Chem. Res. Toxicol. 33 (9), 2324–2337. https://doi.org/10.1021/acs.chemrestox.0c00106.

Lelieveld, J., Evans, J.S., Fnais, M., Giannadaki, D., Pozzer, A., 2015. The contribution of outdoor air pollution sources to premature mortality on a global scale. https://doi.org/10.1038/nature15371.

Liguori, B., Hansen, S.F., Baun, A., Jensen, K.A., 2016. Control banding tools for occupational exposure assessment of nanomaterials - ready for use in a regulatory context? NanoImpact 2, 1–17. https://doi.org/10.1016/j.impact.2016.04.002.

López, M., López Lilao, A., Ribalta, C., Martínez, Y., Piña, N., Ballesteros, A., Fito, C., Koehler, K., Newton, A., Monfort, E., Viana, M., 2022. Particle release from refit operations in shipyards: exposure, toxicity and environmental implications. Sci. Total Environ. 804, 150216. https://doi.org/10.1016/j.scitotenv.2021.150216.

López, M., López-Lilao, A., Romero, F., Pérez-Albaladejo, E., Pinteño, R., Porte, C., Balasch, A., Eljarrat, E., Viana, M., Monfort, E., 2023. Size-resolved chemical composition and toxicity of particles released from refit operations in shipyards. Sci. Total Environ. 880 (March), 163072. https://doi.org/10.1016/j.scitotenv.2023.163072.

Lovén, K., Isaxon, C., Ahlberg, E., Bermeo, M., Messing, M.E., Kåredal, M., Hedmer, M., Rissler, J., 2023. Size-resolved characterization of particles >10 nm emitted to air during metal recycling. Environ. Int. 174, 107874. https://doi.org/10.1016/j.envint.2023.107874.

Markku, K., Pirjola, L., 2001. Development of particle size and composition distributions with a novel aerosol dynamics model. Tellus 53B, 491–509.

Marquart, H., Heussen, H., Le Feber, M., Noy, D., Tielemans, E., Schinkel, J., West, J., Van Der Schaaf, D., 2008. Stoffenmanager. a Web-Based Control Banding Tool Using an Exposure Process Model. Ann. Occup. Hyg 52 (6), 429–441. https://doi.org/10.1093/annhyg/men032.

Matysiak-Kucharek, M., Sawicki, K., Kapka-Skrzypczak, L., 2023. Effect of silver nanoparticles on cytotoxicity, oxidative stress and pro-inflammatory proteins profile in lung adenocarcinoma A549 cells. Ann. Agric. Environ. Med. 30 (3), 566–569. https://doi.org/10.26444/aaem/169214.

Mezquita, A., Boix, J., Monfort, E., Mallol, G., 2014. Energy saving in ceramic tile kilns: cooling gas heat recovery. Appl. Therm. Eng. 65 (1–2), 102–110. https://doi.org/10.1016/j.applthermaleng.2014.01.002.

Minguillón, M. C., Monfort, E., Escrig, A., Celades, I., Guerra, L., Busani, G., Sterni, A., & Querol, X. (n.d.). Air quality comparison between two European ceramic tile clusters. https://doi.org/10.1016/j.atmosenv.2013.04.010.

Nasirzadeh, N., Golbabaei, F., Shekaftik, O.S., 2023. Laboratory activities involving nanomaterials: risk assessment and investigating researchers symptoms. Nanoscale 15 (6), 2674–2689. https://doi.org/10.1039/D2NR06118J.

Oberdörster, G., 2001. Pulmonary effects of inhaled ultrafine particles. Int. Arch. Occup. Environ. Health 74, 1–8.

Oomen, A.G., Steinhäuser, K.G., Bleeker, E.A.J., van Broekhuizen, F., Sips, A., Dekkers, S., Wijnhoven, S.W.P., Sayre, P.G., 2018. Risk assessment frameworks for nanomaterials: scope, link to regulations, applicability, and outline for future

directions in view of needed increase in efficiency. NanoImpact 9 (September 2017), 1–13. https://doi.org/10.1016/j.impact.2017.09.001.
Paik, S.Y., Zalk, D.M., Swuste, P., 2008. Application of a pilot control banding tool for risk level assessment and control of nanoparticle exposures. Ann. Occup. Hyg. 52 (6), 419–428. https://doi.org/10.1093/annhyg/men041.
Pope III, C.A., Dockery, D.W., 2006. Health effects of fine particulate air pollution : lines that connect health effects of fine particulate air pollution : lines that connect. J. Air Waste Manag. Assoc. 56, 709–742. https://doi.org/10.1080/10473289.2006.10464485.
Querol, X., Alastuey, es, Rodriguez, S., Ruiz, C. R., Cots, N., Massagu, G., & Puig, O. (n. d.). Atmos. Environ. 35 (2001) 6407-6419 PM10 and PM2.5 source apportionment in the Barcelona Metropolitan area, Catalonia, Spain.
Rafieepour, A., R Azari, M., Khodagholi, F., 2023. Cytotoxic effects of crystalline silica in form of micro and nanoparticles on the human lung cell line A549. Toxicol. Ind. Health 39 (1), 23–35. https://doi.org/10.1177/07482337221140644.
Reche, C., Viana, M., Moreno, T., Querol, X., Alastuey, A., Pey, J., Pandolfi, M., Prévôt, A., Mohr, C., Richard, A., Artiñano, B., Gomez-Moreno, F.J., Cots, N., 2011. Peculiarities in atmospheric particle number and size-resolved speciation in an urban area in the western Mediterranean: results from the DAURE campaign. Atmos. Environ. 45 (30), 5282–5293. https://doi.org/10.1016/j.atmosenv.2011.06.059.
Ribalta, C., López-Lilao, A., Estupiñá, S., Fonseca, A.S., Tobías, A., García-Cobos, A., Minguillón, M.C., Monfort, E., Viana, M., 2019a. Health risk assessment from exposure to particles during packing in working environments. Sci. Total Environ. 671, 474–487. https://doi.org/10.1016/j.scitotenv.2019.03.347.
Ribalta, C., Viana, M., López-Lilao, A., Estupiñá, S., Minguillón, M.C., Mendoza, J., Díaz, J., Dahmann, D., Monfort, E., 2019b. On the relationship between exposure to particles and dustiness during handling of powders in industrial settings. Annals of Work Exposures and Health 63 (1), 107–123. https://doi.org/10.1093/annweh/wxy092.
Romanowski, H., Bierkandt, F.S., Luch, A., Laux, P., 2023. Summary and derived Risk Assessment of 3D printing emission studies. In: Atmospheric Environment. Elsevier Ltd. https://doi.org/10.1016/j.atmosenv.2022.119501, 294.
Salmatonidis, A., Ribalta, C., Sanfélix, V., Bezantakos, S., Biskos, G., Vulpoi, A., Simion, S., Monfort, E., Viana, M., 2019a. Workplace exposure to nanoparticles during thermal spraying of ceramic coatings, 63(1), 91–106. https://doi.org/10.1093/annweh/wxy094.
Salmatonidis, A., Sanfélix, V., Carpio, P., Pawłowski, L., Viana, M., Monfort, E., 2019b. Effectiveness of nanoparticle exposure mitigation measures in industrial settings. Int. J. Hyg Environ. Health 222 (6), 926–935. https://doi.org/10.1016/j.ijheh.2019.06.009.
Salmatonidis, A., Viana, M., Pérez, N., Alastuey, A., de la Fuente, G.F., Angurel, L.A., Sanfélix, V., Monfort, E., 2018. Nanoparticle formation and emission during laser ablation of ceramic tiles. J. Aerosol Sci. 126 (May), 152–168. https://doi.org/10.1016/j.jaerosci.2018.09.006.
Schlüter, U., Arnold, S., Borghi, F., Cherrie, J., Fransman, W., Heussen, H., Jayjock, M., Jensen, K.A., Koivisto, J., Koppisch, D., Meyer, J., Spinazzè, A., Tanarro, C., Verpaele, S., von Goetz, N., 2022. Theoretical background of occupational-exposure models—report of an expert workshop of the ISES Europe working group “exposure models.”. Int. J. Environ. Res. Publ. Health 19 (3). https://doi.org/10.3390/ijerph19031234.
Sebaugh, J.L., 2011. Guidelines for accurate EC50/IC50 estimation. Pharmaceut. Stat. 10 (2), 128–134. https://doi.org/10.1002/pst.426.
Shin, S.W., Song, I.H., Um, S.H., 2015. Role of physicochemical properties in nanoparticle toxicity. Nanomaterials 5, 1351–1365.
Silva, F., Arezes, P., Swuste, P., 2016. Risk management of occupational exposure to nanoparticles during a development project: a case study. Dyna 83 (197), 9. https://doi.org/10.15446/dyna.v83n197.57584.
Sousa, M., Arezes, P., Silva, F., 2021. Occupational exposure to incidental nanoparticles: a review on control banding. J. Phys. Conf. 1953 (1). https://doi.org/10.1088/1742-6596/1953/1/012008.
Sousa, M., Arezes, P., Silva, F., 2023. Occupational exposure to incidental nanomaterials in metal additive manufacturing: an innovative approach for risk management. https://doi.org/10.3390/ijerph20032519.
Stefaniak, A.B., Bowers, L.N., Knepp, A.K., Virji, M.A., Birch, E.M., Ham, J.E., Wells, J.R., Qi, C., Schwegler-Berry, D., Friend, S., Johnson, A.R., Martin, S.B., Qian, Y., LeBouf, R.F., Birch, Q., Hammond, D., 2018. Three-dimensional printing with nano-enabled filaments releases polymer particles containing carbon nanotubes into air. Indoor Air 28 (6), 840–851. https://doi.org/10.1111/ina.12499.
Stone, V., Nowack, B., Baun, A., van den Brink, N., von der Kammer, F., Dusinska, M., Handy, R., Hankin, S., Hassellöv, M., Joner, E., Fernandes, T.F., 2010. Nanomaterials for environmental studies: classification, reference material issues, and strategies for physico-chemical characterisation. Sci. Total Environ. 408 (7), 1745–1754. https://doi.org/10.1016/J.SCITOTENV.2009.10.035.
Sukhanova, A., Bozrova, S., Sokolov, P., Berestovoy, M., Karaulov, A., Nabiev, I., 2018. Dependence of nanoparticle toxicity on their physical and chemical properties. In: Nanoscale Research Letters, vol. 13. Springer New York LLC. https://doi.org/10.1186/s11671-018-2457-x.
Sushma, Kumar, H., Ahmad, I., Dutta, P.K., 2018. In-vitro toxicity induced by quartz nanoparticles: role of ER stress. Toxicology 404–405, 1–9. https://doi.org/10.1016/j.tox.2018.05.001.
Tokgun, O., Demiray, A., Kaya, B., Karagür, E.R., Demir, E., Burunkaya, E., Akça, H., 2015. Silica nanoparticles can induce apoptosis via dead receptor and caspase 8 pathway on A549 cells. Advances in food sciences 37 (2), 65–70.
Tsai, S.J., Ada, E., Isaacs, J.A., Ellenbecker, M.J., 2009. Airborne nanoparticle exposures associated with the manual handling of nanoalumina and nanosilver in fume hoods. J. Nanoparticle Res. 11 (1), 147–161. https://doi.org/10.1007/s11051-008-9459-z.
UCAR, 2024. Mesoscale & microscale meteorology. https://www.mmm.ucar.edu/models/wrf.
Vaezi-Kakhki, A., Asoodeh, A., 2023. Comparison of different methods for synthesis of iron oxide nanoparticles and investigation of their cellular properties, and antioxidant potential. Int. J. Pharm. 645, 123417. https://doi.org/10.1016/J.IJPHARM.2023.123417.
Van Broekhuizen, P., Van Veelen, W., Streekstra, W.H., Schulte, P., Reijnders, L., 2012. Exposure limits for nanoparticles: report of an international workshop on nano reference values. Ann. Occup. Hyg. 56 (5), 515–524. https://doi.org/10.1093/annhyg/mes043.
Van Duuren-Stuurman, B., Vink, S.R., Verbist, K.J.M., Heussen, H.G.A., Brouwer, D.H., Kroese, D.E.D., Van Niftrik, M.F.J., Tielemans, E., Fransman, W., 2012. Stoffenmanager nano version 1.0: a web-based tool for risk prioritization of airborne manufactured nano objects. Ann. Occup. Hyg. 56 (5), 1–17. https://doi.org/10.1093/annhyg/mer113.
Viana, M., Fonseca, A.S., Querol, X., López-Lilao, A., Carpio, P., Salmatonidis, A., Monfort, E., 2017a. Workplace exposure and release of ultrafine particles during atmospheric plasma spraying in the ceramic industry. Sci. Total Environ. 599–600, 2065–2073. https://doi.org/10.1016/j.scitotenv.2017.05.132.
Viana, M., Fonseca, A.S., Querol, X., López-Lilao, A., Carpio, P., Salmatonidis, A., Monfort, E., 2017b. Workplace exposure and release of ultrafine particles during atmospheric plasma spraying in the ceramic industry. Sci. Total Environ. 599–600, 2065–2073. https://doi.org/10.1016/j.scitotenv.2017.05.132.
Viitanen, A.-K., Uuksulainen, S., Koivisto, A.J., Hämeri, K., Kauppinen, T., 2017. Workplace measurements of ultrafine particles-A literature review. Annals of Work Exposures and Health 61 (7), 749–758. https://doi.org/10.1093/annweh/wxx049.
Voliotis, A., Bezantakos, S., Giamarelou, M., Valenti, M., Kumar, P., Biskos, G., 2014. Nanoparticle emissions from traditional pottery manufacturing. https://doi.org/10.1039/c3em00709j.
Zalk, D.M., Paik, S.Y., Chase, W.D., 2019. A quantitative validation of the control banding Nanotool. Annals of Work Exposures and Health 63 (8), 898–917. https://doi.org/10.1093/annweh/wxz057.
Zalk, D., Paik, S., 2009. Control Banding and Nanotechnology Synergist.
Zhang, Q., Sharma, G., Wong, J.P.S., Davis, A.Y., Black, M.S., Biswas, P., Weber, R.J., 2018. Investigating particle emissions and aerosol dynamics from a consumer fused deposition modeling 3D printer with a lognormal moment aerosol model. Aerosol. Sci. Technol. 52 (10), 1099–1111. https://doi.org/10.1080/02786826.2018.1464115.